Complex Representation in Nonlinear Time Harmonic Eddy Current Problems

Gerhard Paoli and Oszkár Bíró
IGTE, Technical University of Graz, Kopernikusgasse 24, A-8010 Graz, Austria

Gerhard Buchgraber
ELIN Transformatoren GmbH, Elingasse 3, A-8160 Weiz, Austria

Abstract–**Several possibilities are presented to deal with nonlinearity in ferromagnetic media in the case of time harmonic excitation in steady state, without loosing simplicity in describing the potentials by means of complex peak values. The main idea is to introduce a fictitious time independent and inhomogeneous material to take into account the nonlinear relationship between the field quantities. Four methods are shown and investigated on a 3d time harmonic eddy current problem, using the T,Φ-Φ finite element formulation. The vector potential is represented by means of edge elements and the scalar potential by nodal elements. The results obtained are compared with transient computation.**

Index terms–**Eddy currents, 3D, nonlinear media, frequency domain analysis, fictitious material, effective magnetization curve, edge element representation.**

I. Introduction

In linear media, the potentials can be described by their complex peak values assuming that the excitation is time harmonic and steady state is reached. To make use of this complex representation in nonlinear media, too, it is either necessary to regard the fundamental harmonics only (see [13]) or to introduce an effective material. This fictitious material is isotropic and inhomogeneous. It is constant throughout a period and takes into account the nonlinear relationship of the field quantities. It can be described by means of an effective curve. This effective curve shows the nonlinear relationship of the field quantities. In nonlinear magnetic field problems this will be an effective magnetization curve, which originates from the nonlinear B-H curve.

Some methods to create effective magnetization curves are already known from the literature [1]-[6], but for **A**-formulations (based on a magnetic vector potential) and for 1d and 2d field problems only. A review of the different methods to create effective magnetization curves on the basis of the magnetization curve of a ferromagnetic material has been presented by the authors in [7]: it is shown that analogous relations for **T**-formulations (based on a current vector potential) and for **A**-formulations (see [8]) can be obtained for the fictitious material describing the nonlinear behavior of the ferromagnetic material. They are extended to 3d field problems and for **T**-formulations, too and new methods are added. The advantage of all these methods is the very low computation time in comparison to the straightforward transient computation. Both **A**-formulations and **T**-formulations describe with sufficient accuracy the eddy currents in ferromagnetic conducting media and, therefore, the time average of the power losses.

The aim of the authors is to investigate these methods on a highly saturated 3d time harmonic eddy current problem, using the complex formalism and the **T**,Φ-Φ potential formulation [8], [11]. The current vector potential **T** is approximated by means of second order edge shape functions and the magnetic scalar potential Φ by means of second order nodal shape functions. The mapping of the geometry into curvilinear co-ordinates is established with nodal shape functions. The nonlinear, algebraic equations system with complex coefficients, obtained from the differential equations by means of the finite element Galerkin method, is solved by nonlinear iterative techniques [9], [10] and by the conjugate gradient method [15].

II. Fictitious Material

Introducing a fictitious time independent, inhomogeneous material the field quantities can be represented by complex peak values. This means that the corresponding time variation of the components is sinusoidal and hence the peak of the vector representing the physical quantity lies, in general, on the surface of an ellipsoid. The magnitude of the magnetic field intensity, **H,** is given in general as a function of space and time as

$$\begin{aligned} H(\mathbf{r},t) = \big[& H_x^2(\mathbf{r})\cdot\cos^2(\omega t+\varphi_x(\mathbf{r})) \\ & + H_y^2(\mathbf{r})\cdot\cos^2(\omega t+\varphi_y(\mathbf{r})) \\ & + H_z^2(\mathbf{r})\cdot\cos^2(\omega t+\varphi_z(\mathbf{r}))\big]^{1/2}. \end{aligned} \tag{1}$$

In order to create the effective magnetization curve it is sufficient to regard the time dependence $H(t)$ only. $H(t)$ is periodical with $T/2$ and varies between an upper and a lower bound, which depend on the phase angles φ_x, φ_y and φ_z for

Manuscript received November 3, 1997.
Gerhard Paoli, +43 316 873 7756,paoli@igte.tu-graz.ac.at, Oszkár Bíró, +43 316 873 7263, biro@igte.tu-graz.ac.at, fax +43 316 873 7751, http://www.igte.tu-graz.ac.at; Gerhard Buchgraber +43 3172 606 2623, g.buchgraber@etg.elin.at.
This work was supported by Fonds zur Förderung der Wissenschaftlichen Forschung, Vienna, Austria under Grant No. P11291-TEC.

0018-9464/98$10.00 © 1998 IEEE

fixed H_x, H_y and H_z. This means that there are six free parameters for the approximation of $H(t)$ and a family of characteristics of the effective magnetization curves is obtained. However it is sufficient to approximate (1) by

$$H(\mathbf{r},t) = \hat{H}(\mathbf{r})|\cos(\omega t)| \tag{2}$$

arising if $\varphi_x = \varphi_y = \varphi_z$. The magnitude of **B** is then non-sinusoidal

$$B(\mathbf{r},t) = B(H(\mathbf{r},t)) . \tag{3}$$

With (2) and (3) several possibilities exist to create the effective magnetization curves on the basis of the B-H curve. In this paper the methods are shown only for **T**-formulations. For **A**-formulations analogous relations exist.

A. Methods to Construct the Effective Magnetization Curves

1) RMS Method: Assuming (2) to be valid, the effective permeability can be calculated as

$$\mu_{eff} = \frac{B_{RMS}}{H_{RMS}} = \frac{\sqrt{\frac{1}{T}\int_0^T B^2(t)dt}}{\hat{H}/\sqrt{2}} \tag{4}$$

where $B(t)$is obtained from the magnetization curve with (3).

2) DC Method: Similarly to (4),

$$\mu_{eff} = \frac{B_0}{H_0} = \frac{\frac{1}{T}\int_0^T B(t)dt}{\frac{2}{\pi}\hat{H}} \tag{5}$$

where the time averages (DC values) of the field quantities have been used.

3) Simple Energy Method: The following constitutive relation is introduced for **T**-formulations

$$B_{eff} = \mu_{eff}\hat{H} . \tag{6}$$

By means of the magnetic coenergy density, the effective permeability is obtained with (2) and (6) as

$$\mu_{eff} = \frac{2}{\hat{H}^2}\int_0^{\hat{H}} BdH . \tag{7}$$

4) Average Energy Method: The time average coenergy density is defined as

$$\langle w_{co}(t)\rangle^{(t)} = \frac{4}{T}\int_0^{T/4}\left(\int_{H(0)}^{H(t)} BdH\right)dt \tag{8}$$

and with (2) and (6) the effective permeability is

$$\mu_{eff} = \frac{4\cdot\langle w_{co}(t)\rangle^{(t)}}{\hat{H}^2} . \tag{9}$$

The effective magnetization curves are constructed by means of the pairs (H_{RMS}, B_{RMS}), (H_0, B_0) or $(\hat{H}, B_{eff})$. Fig. 1 shows the different effective magnetization curves obtained by the above methods. Different characteristics of the source field quantity are shown on the axes of the diagram.

B. Finite Element Computation

The above methods suggest a general constitutive relation

$$B_{eff}(\mathbf{r}) = \mu_{eff}(\mathbf{r})H_{eff}(\mathbf{r}) \tag{10}$$

which approximates the nonlinear relationship of the field quantities. $H_{eff}(\mathbf{r})$ and $B_{eff}(\mathbf{r})$ are fictitious field quantities in the effective material which is described by the effective magnetization curve. $H_{eff}(\mathbf{r})$ stands for the RMS value, the DC value or the maximal value of $H(\mathbf{r},t)$ in (1) respectively. They are calculated during the finite element computation from (1) as

$$H_{eff}(\mathbf{r}) = \sqrt{\frac{1}{T}\int_0^T H^2(\mathbf{r},t)dt} \quad \text{(RMS method)}, \tag{11}$$

$$H_{eff}(\mathbf{r}) = \frac{1}{T}\int_0^T H(\mathbf{r},t)dt \quad \text{(DC method)}, \tag{12}$$

$$H_{eff}(\mathbf{r}) = \max_t H(\mathbf{r},t) \quad \text{(Energy methods)}. \tag{13}$$

III. POTENTIAL FORMULATION

The field quantities are derived in the **T**,Φ-Φ formulation in the eddy current region (Ω_c) as

$$\mathbf{J} = \nabla\times(\mathbf{T}_0 + \mathbf{T}), \tag{14}$$

$$\mathbf{H} = \mathbf{T}_0 + \mathbf{T} - \nabla\Phi \tag{15}$$

and in the nonconducting region (Ω_n) as

$$\mathbf{H} = \mathbf{T}_0 - \nabla\Phi . \tag{16}$$

$\mathbf{T}_0$ is the impressed vector potential assumed to be given, which models either the current density in the exciting coil or a given total current in a skin effect problem. Several possibilities to choose $\mathbf{T}_0$ are given in [12]. **T** is the reduced current vector potential and Φ is the reduced magnetic scalar potential. **T** is approximated by means of edge elements as

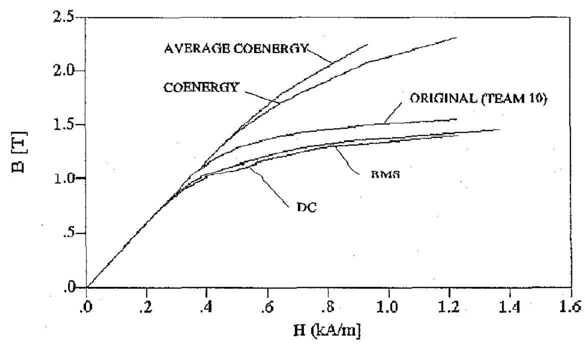

Fig. 1. Effective magnetization curves originated from the magnetization curve in TEAM problem 10.

$$\mathbf{T} = \sum_{k=1}^{N_e} t_k \mathbf{N}_k \tag{17}$$

$$t_k = \int_{edge_k} \mathbf{T} \cdot d\mathbf{s} \tag{18}$$

in the eddy current region and Φ is represented by means of nodal elements as

$$\Phi = \Phi_D + \sum_{k=N_e+1}^{N_e+N_n} \Phi_k N_k \tag{19}$$

in the whole domain. N_e denotes the global number of edges and N_n the global number of nodes. $\mathbf{N}_k$ are the edge shape functions and N_k the nodal shape functions.

The differential equations for the potentials are

$$\nabla \times (\rho \nabla \times \mathbf{T}) - \nabla(\rho \nabla \cdot \mathbf{T}) + \frac{\partial}{\partial t}(\mu \mathbf{T}) - \frac{\partial}{\partial t}(\mu \nabla \Phi) = -\nabla \times (\rho \nabla \times \mathbf{T}_0) - \frac{\partial}{\partial t}(\mu \mathbf{T}_0), \tag{20}$$

$$\nabla \cdot (\mu \mathbf{T} - \mu \nabla \Phi) = -\nabla \cdot (\mu \mathbf{T}_0) \quad \text{in } \Omega_c, \tag{21}$$

$$-\nabla \cdot (\mu \nabla \Phi) = -\nabla \cdot (\mu \mathbf{T}_0) \quad \text{in } \Omega_n. \tag{22}$$

The Coulomb gauge $\nabla \cdot \mathbf{T} = 0$ is incorporated in these equations.

IV. Numerical Investigations

An iron choke with air gaps in the middle core, driven by an exciting coil with a sinusoidal total current of $I = 5.13 \cdot 10^5 A$ at $f = 50Hz$ was modeled. An iron plate with conductivity $\sigma = 4.5 \cdot 10^6 Sm^{-1}$ and thickness $d = 0.015m$ is attached on both sides of the yoke. The material of the choke and the plate are nonlinear. The magnetization curves used are shown in Fig. 3. The curve with the larger slope is valid in the iron choke. In the conducting plate the lower curve, the modified curve of TEAM Problem 10 [16], is used. Fig. 2 shows one eighth of the geometry of the choke with the exciting coil and the finite element mesh of the problem.

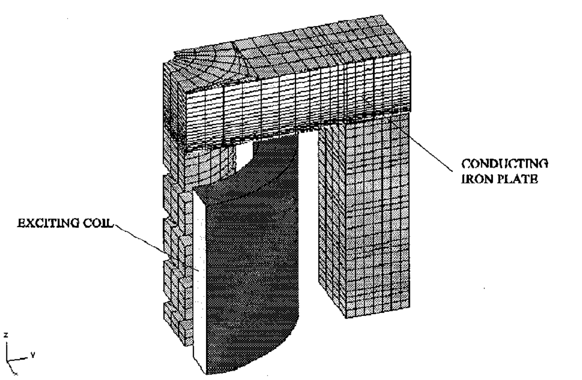

Fig. 2. Finite element model with exciting coil of one eighth of the choke coil.

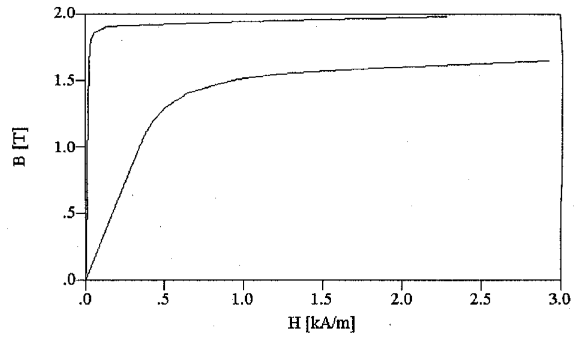

Fig. 3. Magnetization curves of the choke and the conducting plate.

Additionally to the four methods presented above another possibility to deal with the nonlinearity is to use the original magnetization curve in combination with $\max_t H(\mathbf{r},t)$ which is obtained from (1) with (13). These five methods are compared to each other and to a transient computation. Time stepping was carried out over one period with time steps $\Delta t = T/40$. In Table I, the computational efforts of the different methods are compared. Table II shows the time average of the power losses in the conducting plate.

TABLE I: Comparison of CPU Times (s) and Number of Nonlinear Iterations (205 810 Unknowns)

Transient	RMS	DC	Energy	Average	H_{max}
685 790	84 397	79 633	59 229	53 697	162 301
1202 It.	27 It.	21 It.	15 It.	12 It.	112 It.

TABLE II: Time Average of Power Losses in the Plate (W)

Transient	RMS	DC	Energy	Average	H_{max}
107.20	98.63	93.35	84.53	75.91	116.52

Fig. 4 shows the distribution of the current density on the outer side of the iron plate at the time instant $\omega t = 0$ calculated by the RMS method. The same distribution obtained by a transient nonlinear analysis at $t = 0.02s$ is shown in Fig. 5.

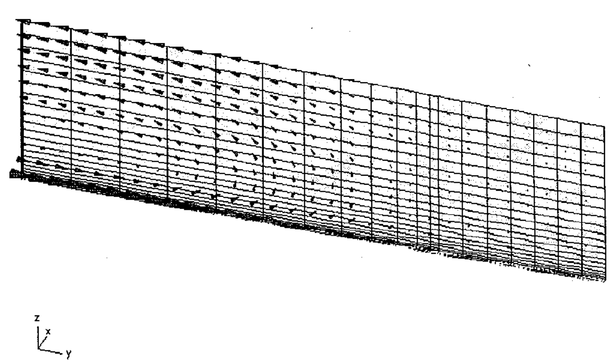

Fig. 4. Distribution of the current density on the conducting plate. RMS method at $\omega t = 0$.

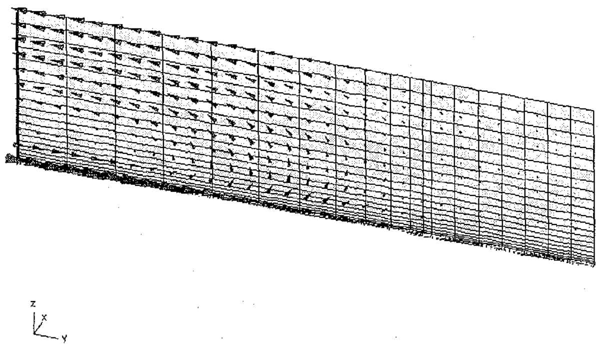

Fig. 5. Distribution of the current density on the conducting plate. Transient computation: $t = 0.02s$.

In Fig. 6, the time functions of the power losses are shown. The RMS method is compared with the solution obtained by the time stepping method. The DC parts of P are $\overline{P} = 107.20W$ for the transient computation and $\overline{P} = 98.63W$ for the RMS method, see Table II.

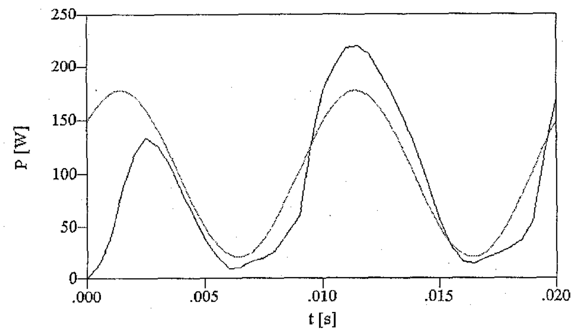

Fig. 6. Power losses during one period in the conducting plate. Transient and approximate sinusoidal time function obtained by the RMS method.

V. Conclusion

All the methods presented show excellent agreement for the power losses and the electric currents with the time consuming transient results. The magnetic fields fit also well. Earlier investigations on a simple eddy current problem, see [7], and the above results give rise to the following conclusion: the RMS and the DC methods work better with **T**-formulations and the energy methods work better with **A**-formulations. The big advantage of all these methods is the substantially lower computational effort.

References

[1] J.D. Lavers, "Finite element solution of nonlinear two dimensional TE-mode eddy current problems," *IEEE Trans Magn. Vol.19*, pp.2201-2203, Sept. 1983.

[2] Y. Du Terrail, Jean-Claude Sabonnadiere, P. Masse and J.L.Coulomb, "Nonlinear Complex Finite Elements Analysis of Electromagnetic Field in Steady-State AC Devices," *IEEE Trans. Magn. Vol.20*, pp.549-552, July 1984.

[3] H. Hedia, J.-F. Remacle, P. Dular, A. Nicolet, A. Genon, W. Legros, "A Sinusoidal Magnetic Field Computation in Nonlinear Materials," *IEEE Trans. Magn. Vol.31*, pp.3527-3529, Nov. 1995.

[4] N.A. Demerdash and D.H. Gillot, "A New Approach for Determination of Eddy Current and Flux Penetration in Nonlinear Ferromagnetic Materials," *IEEE Trans. Magn. Vol.10*, pp.682-685, March 1974.

[5] D. Labridis and P. Dokopoulos, "Finite Element Computation of Eddy Current Losses in Nonlinear Ferromagnetic Sheaths of Three-Phase Power Cables," *IEEE Trans. on Power Delivery Vol.7*, pp.1060-1067, July 1992.

[6] Dieter Lederer and Arnulf Kost, "The Shielding of Underground Cable Systems - Comparison between Calculation and Measurements," *ICEF 96*, October 1996.

[7] Gerhard Paoli and Oszkár Bíró, "Time Harmonic Eddy Currents in Nonlinear Media," to be published in *COMPEL*, 1998.

[8] O. Bíró and K.R. Richter, "CAD in Electromagnetism," in P.W. Hawkes (ed), *Advances in Electronics and Electron Physics*, vol.82, pp.1-96, Academic Press, 1991.

[9] Oszkar Bíró, Kurt Preis and Kurt R. Richter, "Various FEM formulations for the calculation of transient 3d eddy currents in nonlinear media," *IEEE Trans. Magn. Vol.31*, pp.1307-1312, May 1995.

[10] Oszkár Bíró and Kurt Preis, "Finite element calculation of time-periodic 3d eddy currents in nonlinear media," *Advanced Computational Electromagnetics*, T.Honma (Ed.), pp.62-74, IOS Press, 1995.

[11] G. Drago, et al., "A Symmetric Undifferentiated Fully Gauged T,ψ-A-ψ Formulation," *IEEE Trans. Magn. Vol.31*, pp.1352-1355, May 1995.

[12] O. Bíró, K. Preis, W. Renhart, G. Vrisk, K.R. Richter, "Computation of 3D Current Driven Skin Effect Problems Using a Current Vector Potential," *IEEE Trans. Magn. Vol.29*, pp.1325-1328, March 1993.

[13] Sotoshi Yamada, Paul P. Biringer and Kazuo Bessho, "Calculation of Nonlinear Eddy Current Problems by the Harmonic Balance Finite Element Method," *IEEE Trans. Magn. Vol.27*, pp.4122-4125, Sept. 1991.

[14] R. Harrington, *Time Harmonic Electromagnetic Fields*, New York, McGraw-Hill, 1961, ISBN 07-026745-6.

[15] H.R. Schwarz, *Methode der finiten Elemente*, B.G. Teubner Stuttgart 1984, Kapitel 4, pp.212-232.

[16] Takayoshi Nakata and Koji Fujiwara, "Results for Benchmark Problem 10 (Steel Plates Around a Coil)," *COMPEL Vol.9 No.3*, pp.181-190, Sept. 1990.